



## Layout optimization for renovation of operational offshore wind farm based on machine learning wake model

Kun Yang, Xiaowei Deng\*

Department of Civil Engineering, The University of Hong Kong, Pokfulam, Hong Kong



### ABSTRACT

In the past, offshore wind farms commonly had a large wind turbine distance to avoid power loss induced by the wake effects. For this reason, the operational offshore wind farms with such a large wind turbine distance are relatively low in capacity density and have a great potential to include more wind turbines. This paper aims to provide a suitable renovation plan for those operational wind farms. Different from traditional wind farm layout optimization, the purpose of the renovation is to install new wind turbines while maintaining the status quo, which is an optimization problem with the constraint of initial wind turbines. Therefore, the renovation plan can be applied flexibly without waiting for the decommissioning of initial wind turbines. In this paper, the renovation plan is provided by a robust wind farm layout optimization framework based on a machine learning wake model, which can evaluate overall power production more accurately than traditional analytical models. Both heuristic and gradient-based optimization algorithms are applied and compared. Horns Rev wind farm is analyzed for demonstration. The differences between the two algorithms are limited to 1%. Furthermore, the renovation and freeform optimizations are successfully applied to the cases with 12.5%~50% more wind turbines. According to the results, the freeform optimizations without the constraint of initial wind turbines have similar performance to renovation plans with an error smaller than 0.3%. When the number of wind turbines is added from 80 to 120, the normalized AEP (annual energy production) slightly decreases from 96.6% to 93.4%, which means the power loss increases by 3%~4%. In the meantime, the capacity density increases significantly by 50% as the area remains the same. In conclusion, the renovation plan is recommended for aging wind farms with a low capacity density like Horns Rev wind farm.

### 1. Introduction

Wind energy is one of the most promising renewable energy sources (Nazir et al., 2019; Wang and Wang, 2015), which is indispensable in the race to reach the Paris Agreement goal of 1.5 °C global warming (Global wind energy council, 2022). Wind energy has pronounced advantages: pollution-free, no greenhouse gas emissions, sustainable, cost-effective, etc. Thus, wind energy is a sound choice to reach the net-zero emission targets, which have been set or are under-considered by over 100 countries (Van Soest et al., 2021). Overall, wind power is a favorable choice and an essential component of global sustainable development. As a result, the wind market keeps in rapid development on a global scale. In principle, the installed capacity is used to represent the development status of wind power. According to the latest report (Global wind energy council, 2022), wind energy development has continuously increased for decades with significant growth (Fig. 1). Particularly, offshore wind energy is becoming popular and developing vigorously. As shown in Fig. 2, the new wind power capacity added worldwide in 2021 was as high as 93.6 GW. The global installed wind capacity has increased to 837 GW in total, indicating a great growth of 12.4% in the passing year. In addition, among the newly installed

capacity, 72.5 GW was installed onshore. As shown in Fig. 2, the added onshore capacity in 2021 is smaller than 2020 but still the second-highest in history. Meanwhile, the offshore wind capacity has a record year with a new installation of over 21 GW. The added offshore capacity in 2021 is three times larger than that in 2020, which marks a new trend in wind power development.

The growth of offshore wind power is significant. Meanwhile, it brings more challenges and requirements for advanced technologies. Particularly, the offshore wind farms layout is usually in empirical rectilinear grids (Lackner and Elkinton, 2007), also called 'regular grids' or 'in array' (Elkinton et al., 2008; Gao et al., 2016; Hou et al., 2019; Kusiak and Song, 2010; Pillai et al., 2015). As the total capacity of an offshore wind farm is growing large rapidly, even small optimal ratios will make large profits (Hou et al., 2019). Wind farm layout optimization is a sound choice to change the locations of wind turbines to avoid large power loss induced by turbine wakes (Gao et al., 2015; Guo et al., 2021; Pérez-Aracil et al., 2022). However, many large-scale offshore wind farms have already been constructed and operating for years. In this case, the research about end-of-life strategies and repowering is also extensive, which are mainly about the decommissioning of the old wind turbines after over 20 operational years and installation of new wind

\* Corresponding author.

E-mail address: [xwdeng@hku.hk](mailto:xwdeng@hku.hk) (X. Deng).

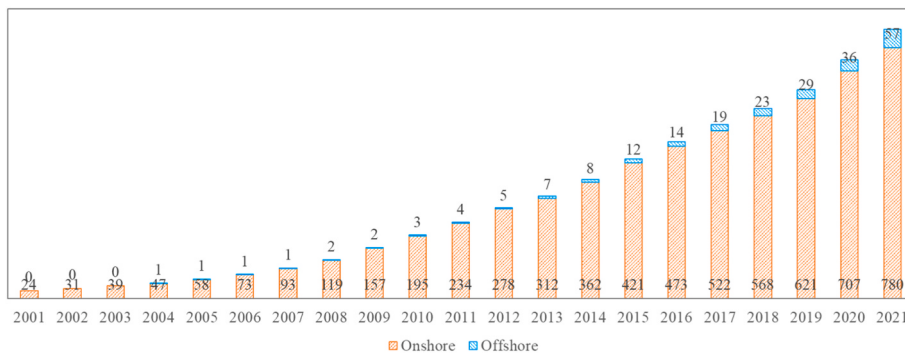


Fig. 1. Total installed capacity in this century (GW).



Fig. 2. New installed capacity in this century (GW).

turbines. Therefore, these strategies can only be applied at the end of the wind farms' life.

As a branch of spatial optimization, wind farm layout optimization (WFLO) has become a hot topic by optimize the locations of wind turbines in the design stage of a wind farm (Wang et al., 2015, 2018; Yang et al., 2018). The optimization algorithms adopted in WFLO can be summarized in two mainstream: gradient-based and gradient-free methods. Among gradient-free methods, heuristic algorithms are more popular than others. Early in 1994, Mosetti proposed an optimization scheme based on genetic algorithms (Mosetti et al., 1994). In the scheme, the area is discretized into grids, which matches the problem formulation requirements of genetic algorithm. Later Particle Swarm Optimization (PSO) becomes popular and widely-adopted (Tao et al., 2020b; Wan et al., 2010). Those heuristic algorithms along with gradient-based methods are all summarized in many reviews (Balasubramanian et al., 2020; González et al., 2014; Hou et al., 2019; Tao et al., 2020a).

In this paper, a new strategy is provided as an alternative: a renovation of the wind farm while maintaining the initial wind turbines. The layout of newly added wind turbines is optimized with the constraint of initial wind turbines. Different from wind farm extension, no extra wind farm area is required. In the meantime, the construction of additional wind turbines has limited impact on initial wind turbines, so the renovation plan can be flexibly applied during the whole operation stage of the offshore wind farms. Therefore, the initial wind turbines can keep operating normally until the end of their lives, while the capacity density and annual energy production can increase significantly.

## 2. Methodology

### 2.1. Numerical modeling of turbine wake

Wind turbine wakes are widely modeled by turbulence models in computational fluid dynamics (CFD). The  $k - \varepsilon$  model and  $k - \omega$  model

are two popular RANS models to properly resolve the areas far and near the wall, respectively. Two-equation standard  $k - \varepsilon$  turbulence model is suitable for mean flow characterization, such as mean wind speed. A modified  $k - \varepsilon - f_p$  model is proposed by M. van der Laan (van der Laan et al., 2013). The  $k - \varepsilon - f_p$  model can correct the viscosity parameter to have more accuracy results, and its robustness has been well validated in literature (Ti et al., 2020; Van Der Laan et al., 2015). The problem in this paper is a large-scale wind turbine modeling under atmospheric boundary layer (ABL) conditions. Particularly, wind farm power is mainly affected by mean flow characteristics (Blocken et al., 2007). Therefore, the  $k - \varepsilon - f_p$  model is adopted in the numerical simulation in this paper, along with proper ABL condition. Apart from the turbulence model, the wind turbine should also be modeled. However, full-scale modeling is too computationally expensive. A reduce-order model named the Actuator-disk model (ADM) is widely used to simulate the wind turbine rotor. Particularly, an Actuator-disk model with rotation (ADM-R) is extended from the traditional ADM. The ADM-R model is proved to be more efficient and accurate in wind turbine simulation (Wu and Porté-Agel, 2015). The ADM-R method specifies a thin virtual disk with the same surface area as the rotor swept area. The lift and drag forces induced by the rotor in this area are calculated using the blade element method (BEM). The method is well-developed, and its detailed introduction can be found in (El Kasmi and Masson, 2008; Göçmen et al., 2016; Javaherchi et al., 2014; Ti et al., 2020; Wu and Porté-Agel, 2015).

### 2.2. Machine learning wake model based on CFD simulation

In this study, a machine learning wake model is developed and adopted to solve the wake effects instead of analytical wake models in optimization. Commonly, the wake model can be evaluated millions of times in an optimization. Therefore, the current commercial software is usually equipped with efficient analytical wake models, such as the Park model and Gaussian wake model. Apart from those choices, a machine learning wake mode is better with the same accuracy as numerical

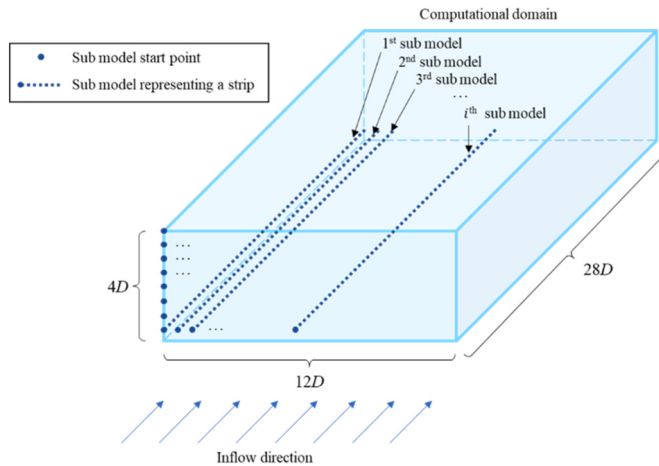


Fig. 3. Schematics of sub-models of machine learning wake model.

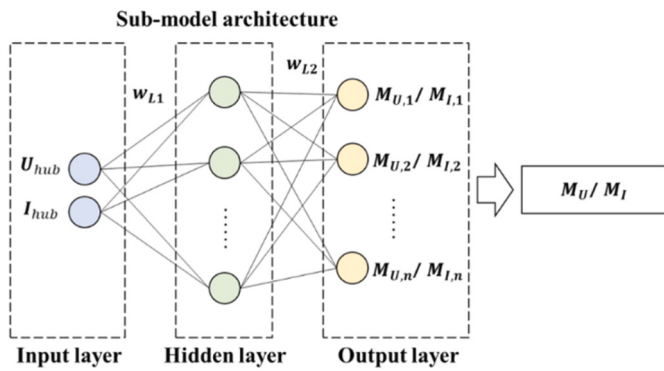


Fig. 4. Architecture of a sub-model of machine learning wake model.

simulation and sufficient efficiency for optimization.

### 2.2.1. Database preparation

First, an accurate dataset is essential because it represents the upper bound of model accuracy. Therefore, a rigorously validated CFD simulation method is adopted to generate the dataset. In the dataset, hundreds of cases are included, which should cover the whole possible operating conditions of the wind turbine. In this study, the study case is about the Horns Rev wind farm. For example, the Vestas V80 2 MW wind turbine installed in this wind farm has a range of operating conditions, whose inflow velocity is from 5 m/s to 20 m/s. In the meantime, the turbulence intensity of the ambient wind at Horns Rev wind farm is around 7%–8%. However, the turbulence intensity may achieve over 20% in the turbine wake for downstream wind turbines. Therefore, the database is defined to have a wide coverage: 5 m/s~20 m/s for inflow velocity and 2%~30% for turbulence intensity at hub height. With a spacing of 0.5 m/s and 2% for velocity and turbulence intensity, the total number of cases is  $31 \times 15 = 465$ . It should be noticed that the wind turbine is operating in its proper status in each case following the completed control curves, including rotor speed control and blade pitch control. The method includes those key factors in realistic operation, which guarantee the accuracy of CFD simulation.

### 2.2.2. Machine learning wake model

When the database is ready, an Artificial Neural Network can be established. The optimization requires efficient responses, which means the wake model's evaluation time should be as short as possible. Therefore, machine learning methods with a complicated framework and many parameters are impossible to adopt. In this case, the simplest

Table 1

Distribution of cases.

	Wind speed (m/s)	Number of cases	Training cases	Testing cases
Low-speed region	5–10	165	143	22
High-speed region	10–20	315	293	22

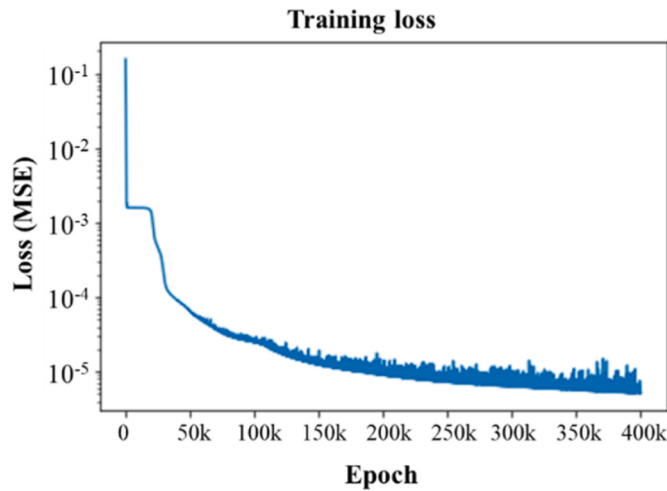


Fig. 5. Training loss (mean square error) versus epoch.

machine learning model, an ANN framework with a single hidden layer, is used in this study. The whole domain is large enough for wake analysis with a length of  $28D$ . As the rotor diameter ( $D$ ) of Vestas V80 2 MW wind turbine is 80m, the computational domain is 960m wide, 320m high, and 2240m long in this study. Moreover, the computational domain is also divided into 'Strips' as shown in Fig. 3. The spacing of start points is 10m, which means 97 grid points on horizontal and 32 grid points on vertical with the ground being skipped. Therefore, the machine learning wake model has 3104 sub-models for the velocity model and turbulence model, respectively.

The architecture of each sub-model is demonstrated in Fig. 4. The velocity models and turbulence intensity models share the same architecture. The layer number is defined as one to ensure an efficient framework, while the best learning rate is found to be 0.01, and the layer size is the same as that in literature (Ti et al., 2020, 2021).

A python-based API interface, Keras, assists in modeling each sub-model. Tensorflow is applied as the backend. After preliminary tests, the best architecture consists of an input layer with two variables, a hidden layer with the 'tanh' activation function  $f_1(x)$ , and an output layer with the Rectified Linear Unit activation function  $f_2(x)$ . The activation functions are as follows:

$$f_1(x) = \tanh(x) = \frac{2}{1 + e^{-2x}} - 1 \quad (1)$$

$$f_2(x) = \max(x, 0) \quad (2)$$

### 2.2.3. Overfitting issue and case separation

Overfitting is one of the most significant issues in machine learning. Therefore, independent testing datasets are extracted, while the rest of the cases are used for training. As the number of datasets is relatively limited, 22 testing cases are evenly selected for each wind speed region. Detailed information about the distribution of cases is shown in Table 1. The testing cases will not be involved during the whole training procedure. After training, the trained machine learning model will be used to predict the testing cases. As the testing cases are independent, the

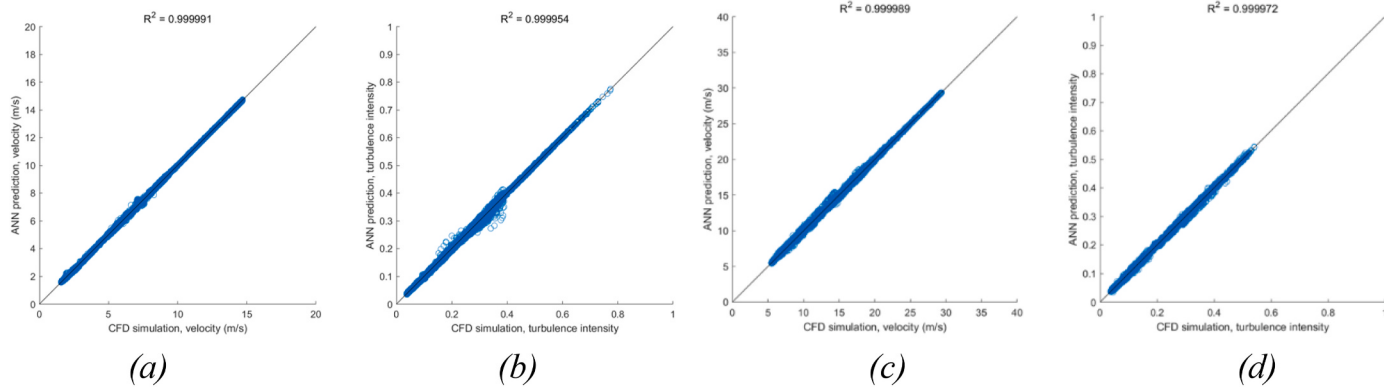


**Fig. 6.** Correlation analysis (a) low-speed region, velocity model (b) low-speed region, turbulence intensity model (c) high-speed region, velocity model (d) high-speed region, turbulence intensity model.

results will be able to check whether the model is overfitted or not.

#### 2.2.4. Model training

The optimizer and number of epochs are also investigated in preliminary tests. As a result, optimizer ‘Adam’ is found to be the most efficient, while 40000 epochs are enough and suitable for training.

The history of training loss is shown in Fig. 5. According to the figure, the mean square error decreases rapidly at the beginning. When the epoch is between 300k to 400k, the performance of the model becomes very stable and reliable. However, training loss cannot prove the effectiveness of the model. Therefore, the trained model will be applied to predict the test cases and compared with the CFD simulation results.

#### 2.2.5. Testing results

As mentioned in Table 1, about 10% of cases are reserved for testing, which is not involved in the training process. In this case, the prediction results can evaluate the trained model’s accuracy and check whether the model is overfitted.

The correlation analysis is applied between CFD simulation results and ANN prediction results. The scatter plots and coefficient of determination are shown in Fig. 6. The coefficient of determination in each case is very high, representing a high agreement between ANN prediction and CFD simulation. Moreover, the trained models have no overfitting issues. In this way, the machine learning model can be used to efficiently predict the wake effects with high accuracy as the CFD simulation.

### 2.3. Wake superposition method

Wake superposition methods are widely used in multiple wind turbine cases. The wake effects behind multiple wind turbines can be effectively evaluated using proper equations called wake summation or wake superposition. The related methods are well developed and can be found in the literature (Göçmen et al., 2016; Kuo et al., 2014; Ti et al., 2020). According to the authors’ review, proper velocity and turbulence intensity summation methods are selected, respectively:

$$\left(1 - \frac{u_i}{u_\infty}\right)^2 = \sum_{j=1}^{N_{WT}} \left(1 - \frac{u_{ij}}{u_j}\right)^2 \quad (3)$$

$$k_i - k_\infty = \sum_j^{N_{WT}} \Delta k_{ij} \quad (4)$$

where  $N_{WT}$  is the number of wind turbines,  $u$  and  $k$  are the velocity and turbulence intensity at the hub height, respectively. Subscripts  $\infty, i, j$  denote the location at the inlet, downstream wind turbine, and upstream wind turbine, respectively. Particularly,  $u_{ij}$  and  $\Delta k_{ij}$  represent the ve-

locity and added TKE of downstream wind turbine  $i$  induced by upstream wind turbine  $j$ .

### 2.4. Optimization algorithms

In the past, it has been pointed out that the wind farm layout optimization problem is complicated and highly nonlinear (Elkinton et al., 2008). Therefore, some researchers recommend gradient-free algorithms, such as the Genetic Algorithm (GA) and Particle Swarm Optimization algorithm (PSO) (Brogna et al., 2020; Elkinton et al., 2008). In this study, both gradient-free algorithms and gradient-based algorithms are applied for a comprehensive analysis. The GA method and SQP gradient-based method are applied to represent gradient-free algorithms and gradient-based algorithms, respectively. For better comparison, both methods are applied on the MATLAB platform, which has complete introductions for both algorithms (The MathWorks Inc, 2022a, b). Particularly, multi-start method has been adopted in SQP gradient-based method to find the minimum of multiple local minimums. Moreover, the population in GA is defined as the same of random start points in SQP, which is 200 as suggested in MATLAB guide. The stopping criteria will be checked including the improvement of objective function, step length. As the coordinates will be scaled to [0,1] for normalization, the tolerances are all set as  $1 \times 10^{-6}$ . Even a maximum iteration limit is set for both algorithms. The programs terminated because of the objective function changes smaller than the criterion.

## 3. Optimization problem scheme

### 3.1. A general optimization problem setup

In the past, the wind farm layout optimization was usually simplified using Mosetti’s problem scheme (Mosetti et al., 1994), in which the area is divided into discrete grids, and the wind turbines are only located at the centers of grids. This simplification significantly reduces the probabilities of layout designs. Later, some researchers also tried coordinate models, which directly apply the coordinates as variables (Kusiak and Song, 2010). This issue has been well reviewed in reviews (González et al., 2014; Hou et al., 2019). In this study, a coordinate model will be optimized for a large-scale wind farm with 80 or more wind turbines. Therefore, the variables in this problem will be 160 or more, which will bring challenges to the efficiency of the local solver and the optimization algorithm.

The local solver is the method adopted to evaluate the annual energy production (AEP) of the wind farm, which can be expressed as Eq. (5):

$$AEP = T_y \sum_{i=1}^{N_s} P_i \bullet f_i \quad (5)$$

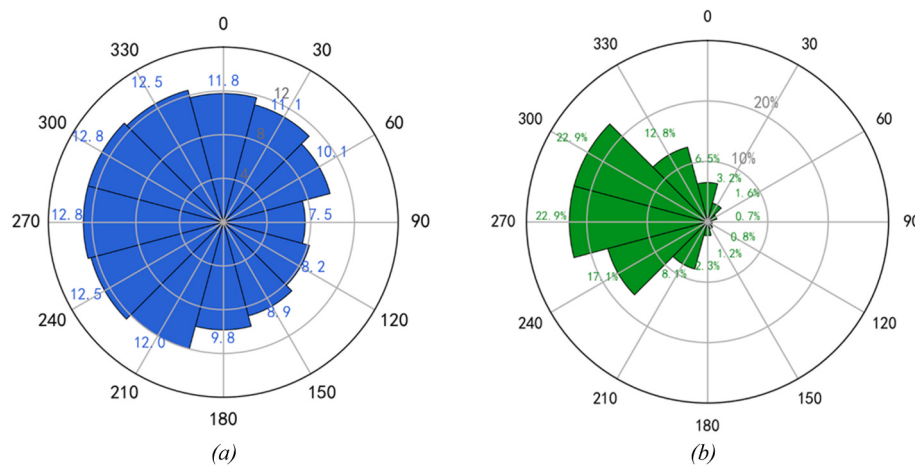


**Fig. 7.** (a) Mean wind speed and (b) probability of wind condition at Horns Rev wind farm during 2019–2021.

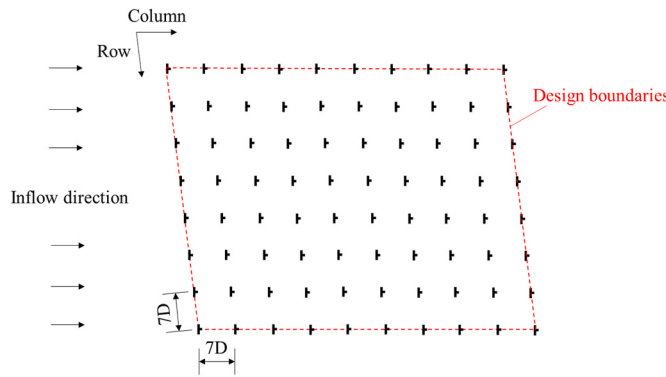


**Fig. 8.** Schematics of Horns Rev offshore wind farm initial layout design.

where  $T_y$  represents the time of one year, which is 8760 h,  $N_s$  is the number of sectors,  $P_i$  and  $f_i$  denotes the power production and probability of  $i$  th wind sector, respectively.

### 3.2. Inflow conditions

In order to obtain a more realistic prediction on AEP, the inflow condition should be as detailed as possible. On the other hand, the number of wind speed intervals and the number of sectors will determine the computational cost of the optimization. After balancing these two points, the wind rose is defined with 12 sectors. Mean wind speed of three years (2019–2021) is used in every wind sector. The wind speed data is based on an online database provided by Copernicus Climate Change Service (C3S) Climate Data Store (CDS). The dataset ‘ERA5 hourly data on single levels from 1979 to present’ (Hersbach et al., 2018) contains hourly global wind data. Meanwhile, an average turbulence intensity of 8% is defined for all the cases. After extracting wind data at Horns Rev wind farm location, the mean wind speed at hub height (70 m) and the probability distribution are shown in Fig. 7. The nearest three full years (2019–2021) are investigated.

### 3.3. Horns Rev wind farm initial design

Horns Rev offshore wind farm consists of 80 Vestas V80 2 MW wind turbines. Its current layout is shown in Fig. 8. As the original design boundary can hardly be found, the design boundaries are defined as the envelope of the initial layout. The initial spacing is  $7D$ , which is a long distance with limited wake effects.

**Table 2**

Capacity density of Horns Rev wind farm with different number of wind turbines.

Horns Rev wind farm				
Area (km <sup>2</sup> )	19.61			
Number of WT	80	90	100	120
Capacity of single WT (MW)	2	2	2	2
Capacity (MW)	160	180	200	240
Capacity density (MW/km <sup>2</sup> )	8.16	9.18	10.20	12.24

### 3.4. Renovation optimization and freeform optimization

The renovation plan proposed in this paper means constructing additional wind turbines within the operational wind farm. Therefore, the variables are the coordinates of additional wind turbines. In the meantime, all the initial wind turbines will remain the same. The renovation cases have 10, 20, and 40 additional wind turbines. The gradient-based algorithm combined with the multi-start global optimization method is adopted in the optimization, and so is the genetic algorithm.

The freeform optimization means the overall wind farm is assumed to be reconstructed. Therefore, the locations of all wind turbines are optimized within the design boundaries. This case is a normal wind farm layout optimization (WFLO). The freeform cases are defined with the same number of wind turbines as renovation cases. Therefore, the freeform cases have 90, 100, and 120 wind turbines.

### 3.5. Results and discussion

#### 3.5.1. Initial design

The initial design of the Horns Rev wind farm is first investigated. Its annual energy production (AEP) is evaluated under the wind condition demonstrated in Fig. 7. For normalization, the AEP of the initial design is divided by the AEP of an equivalent number of wind turbines without wake effects. The normalized AEP of the initial layout is  $\bar{P}_{0,nw} = 96.6\%$ , which means the initial design of the Horns Rev wind farm has a limited optimal potential with only a little wake effect. Conducting layout optimization can only achieve a maximum optimal ratio of  $r_{max} = (1/0.966 - 1) = 3.57\%$ .

#### 3.5.2. Results of renovation and freeform optimization

As mentioned above, the spacing of the initial design of the Horns Rev wind farm is large enough with only a little wake effect. The large spacing will ensure the performance of the wind farm, but it requests more area. The capacity density of Horns Rev is relatively small, with

**Table 3**

Normalized AEP of wind farm.

Number of WTs	Renovation plan	
	GS	GA
90	95.7%	95.9%
100	94.9%	95.0%
120	93.1%	93.4%

only 8.16 MW/km<sup>2</sup>, as shown in [Table 2](#). Note that the coverage of design boundaries in [Fig. 8](#) is assumed to be the area. When the number of wind turbines increases, the capacity density grows linearly because no more area is required. Under this circumstance, the cases with additional wind turbines are optimized with two different plans: renovation and freeform. The renovation plan remains the initial layout,

while the freeform plan optimizes the locations of all the wind turbines. The results of optimal designs are shown in [Figs. 9–11](#). GS denotes the gradient search optimization method, and GA represents the Genetic Algorithm method (see [Table 3](#)).

The optimal layouts seem to have no regulation when the number of additional wind turbines is only 10. However, when 20 and 40 additional wind turbines are added, the locations of them are mainly concentrated in the right part of the area. It is because the mainstreams of the wind rose are Westerly and Northwesterly winds, according to [Fig. 7](#). When most additional wind turbines are located in the right part, the turbine wakes will affect fewer wind turbines.

During optimization, the objective function becomes flat near the optimal solution. The step becomes very small, and the objective function drops slowly. Therefore, GS is more likely to stop early. Anyhow, the optimal solutions searched by both methods all have good

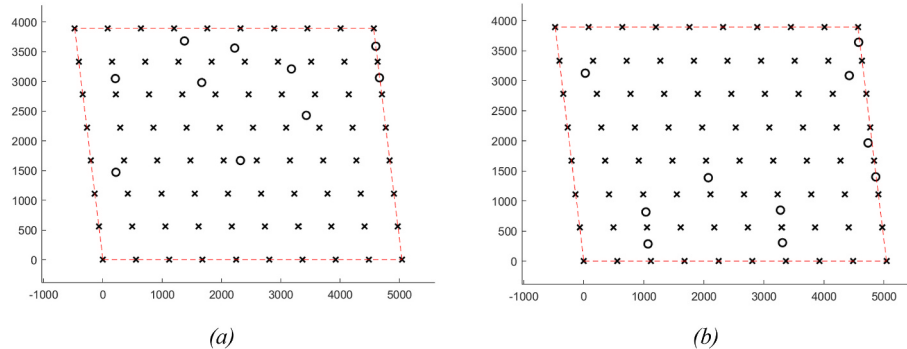


**Fig. 9.** Optimal layout of renovation plan with 10 additional wind turbines (a) GS method; (b) GA method (Cross: initial wind turbine; Circle: additional wind turbine).

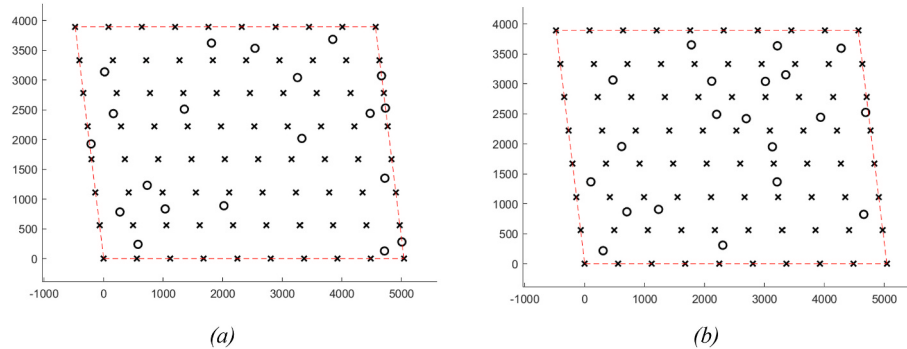


**Fig. 10.** Optimal layout of renovation plan with 20 additional wind turbines (a) GS method; (b) GA method (Cross: initial wind turbine; Circle: additional wind turbine).

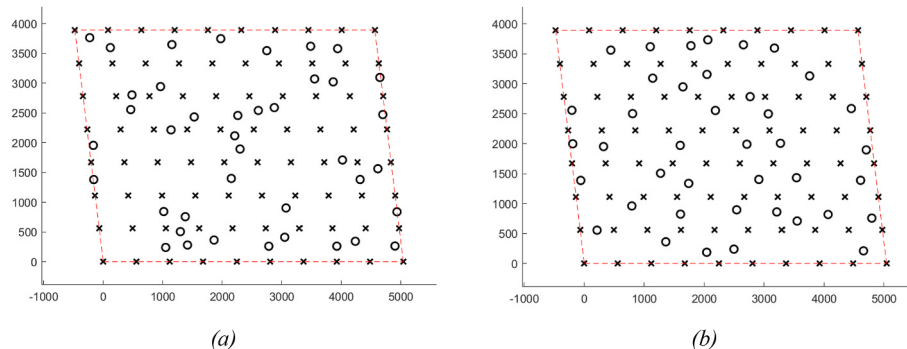


**Fig. 11.** Optimal layout of renovation plan with 40 additional wind turbines (a) GS method; (b) GA method (Cross: initial wind turbine; Circle: additional wind turbine).

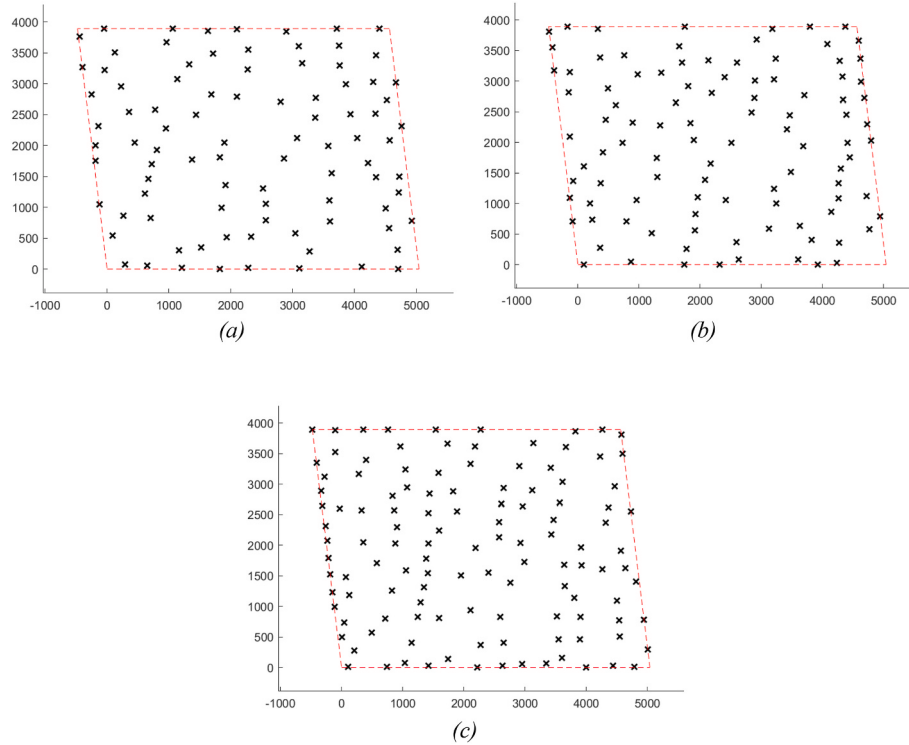


**Fig. 12.** Optimal layout of freeform plan with (a) 90 WTs (b) 100 WTs (c) 120 WTs using GS method.

**Table 4**  
Normalized AEP of optimal layouts with freeform plan.

Freeform plan			
Case	(a)	(b)	(c)
Number of WTs	90	100	120
$\bar{P}$	95.4%	94.3%	93.7%

performances. The error between them is limited to 0.3%. Therefore, both methods are reliable for finding an optimal solution with good performance. As the results are all close to the optimal limits, it is believed that the optimal solution is close to the global minimum, and the optimal algorithms will not make significant differences.

Besides, the freeform plan is also optimized. The optimal layouts of the freeform plan are shown in Fig. 12, and the results are shown in Table 4. The optimal layouts of the freeform plan are lower than the renovation plan with 90 and 100 wind turbines. The results are mainly due to the limited optimal potential. The gradient search method tends to have very small steps for each iteration under this circumstance. When the number of wind turbines is determined, the distances between optimal solutions from different cases are all smaller than 1%. Therefore, the optimal results are good enough, and the function evaluation is close to the global minimum.

When the number of wind turbines grows to 120, the wake effects become larger than before, which also represents larger optimal potential. In this case, the freeform plan of the entire wind farm can easily have an optimal solution with better performance (93.7%) than the renovation plan (93.4%).

#### 4. Conclusions

This study uses a machine learning wake model instead of analytical models in the optimization framework. The modeling of the machine learning wake model is introduced. The accuracy of the machine learning wake model is proved to be at the same level as CFD simulation.

With such an accurate and efficient wake model, renovation and layout optimization of Horns Rev wind farm cases are investigated. The wind data covering 2019 to 2021 at Horns Rev wind farm is summarized. Under this wind condition, the initial layout of the Horns Rev wind farm has limited wake effects. The normalized AEP is 96.6%, and the power loss is only 3.4%. As a result, the wind farm has little optimal potential in normal layout optimization. On the other side, the large spacing of the initial layout denotes a low level of capacity density in this wind farm.

As Horns Rev wind farm has been operating for nearly 20 years, the wind farm becomes aging. At this stage, it is suggested in this paper that more wind turbines can be added. The capacity density can rise from  $8.16 \text{ MW/km}^2$  to  $12.24 \text{ MW/km}^2$  when the number of wind turbines grows from 80 to 120. Meanwhile, the power loss will not significantly enlarge if proper plans are applied. This paper discusses two plans for additional wind turbines: the renovation plan and the freeform plan. In the study cases, the number of wind turbines is added from 80 to 120. The initial wind turbines remained the same in the renovation plan, which has a good performance with a normalized AEP of 93%–96%. In other words, the power loss increases only 3%–4% when the number of wind turbines (and capacity density) grows by 50%. The operational lifetime of wind turbines is around 20–25 years. A renovation plan can be applied to wind farms at any time. As the results of the renovation plan and the freeform plan are close, the renovation plan seems to be a better choice due to its high flexibility for designers.

In the future, machine learning techniques can be applied more widely in wind energy, especially wake modeling. Wake steering, or yaw control, becomes the efficient way in operational stage of wind farm, the wake of a yawed wind turbine wake has the possibility to be formulated with a machine learning model.

#### CRediT authorship contribution statement

**Kun Yang:** Methodology, Investigation, Validation, Visualization, Writing – original draft. **Xiaowei Deng:** Conceptualization, Funding acquisition, Supervision, Writing – review & editing.

## Declaration of competing interest

The authors declare that they have no known competing financial interests or personal relationships that could have appeared to influence the work reported in this paper.

## Data availability

No data was used for the research described in the article.

## Acknowledgment

The computations were performed using research computing facilities offered by Information Technology Services, the University of Hong Kong. This work is generously supported by the Research Grants Council via RGC/CRF (C7038-20GF) and RGC/GRF (17204122), Shenzhen Science and Technology Innovation Committee via Fundamental Research General Program (2021302011), and National Natural Science Foundation of China via General Program (Project No. 51878586).

## References

- Balasubramanian, K., Thanikanti, S.B., Subramaniam, U., Sudhakar, N., Sichilalu, S., 2020. A novel review on optimization techniques used in wind farm modelling. *Renew. Energy Focus* 35, 84–96.
- Blocken, B., Carmeliet, J., Stathopoulos, T., 2007. CFD evaluation of wind speed conditions in passages between parallel buildings—effect of wall-function roughness modifications for the atmospheric boundary layer flow. *J. Wind Eng. Ind. Aerod.* 95, 941–962.
- Brogna, R., Feng, J., Sørensen, J.N., Shen, W.Z., Porté-Agel, F., 2020. A new wake model and comparison of eight algorithms for layout optimization of wind farms in complex terrain. *Appl. Energy* 259, 114189.
- El Kasmi, A., Masson, C., 2008. An extended k-e model for turbulent flow through horizontal-axis wind turbines. *J. Wind Eng. Ind. Aerod.* 96, 103–122.
- Elkinton, C.N., Manwell, J.F., McGowan, J.G., 2008. Algorithms for offshore wind farm layout optimization. *Wind Eng.* 32, 67–84.
- Gao, X., Yang, H., Lin, L., Koo, P., 2015. Wind turbine layout optimization using multi-population genetic algorithm and a case study in Hong Kong offshore. *J. Wind Eng. Ind. Aerod.* 139, 89–99.
- Gao, X., Yang, H., Lu, L., 2016. Optimization of wind turbine layout position in a wind farm using a newly-developed two-dimensional wake model. *Appl. Energy* 174, 192–200.
- Global wind energy council, 2022. Global Wind Report 2022.
- Göçmen, T., Van der Laan, P., Réthoré, P.-E., Diaz, A.P., Larsen, G.C., Ott, S., 2016. Wind turbine wake models developed at the technical university of Denmark: a review. *Renew. Sustain. Energy Rev.* 60, 752–769.
- González, J.S., Payán, M.B., Santos, J.M.R., González-Longatt, F., 2014. A review and recent developments in the optimal wind-turbine micro-siting problem. *Renew. Sustain. Energy Rev.* 30, 133–144.
- Guo, N., Zhang, M., Li, B., Cheng, Y., 2021. Influence of atmospheric stability on wind farm layout optimization based on an improved Gaussian wake model. *J. Wind Eng. Ind. Aerod.* 211, 104548.
- Hersbach, H., Bell, B., Berriesford, P., Biavati, G., Horányi, A., Muñoz Sabater, J., Nicolas, J., Peubey, C., Radu, R., Rozum, I., Schepers, D., Simmons, A., Soci, C., Dee, D., Thépaut, J.-N., 2018. ERA5 hourly data on single levels from 1979 to present. In: CDS in: (CDS), C.C.C.S.C.S.C.D.S. (Ed.).
- Hou, P., Zhu, J., Ma, K., Yang, G., Hu, W., Chen, Z., 2019. A review of offshore wind farm layout optimization and electrical system design methods. *J. Mod. Power Syst. Clean Energy* 7, 975–986.
- Javaherchi, T., Anteame, S., Aliseda, A., 2014. Hierarchical methodology for the numerical simulation of the flow field around and in the wake of horizontal axis wind turbines: rotating reference frame, blade element method and actuator disk model. *Wind Eng.* 38, 181–201.
- Kuo, J.Y., Romero, D.A., Amon, C.H., 2014. A novel wake interaction model for wind farm layout optimization. American Society of Mechanical Engineers. In: ASME International Mechanical Engineering Congress and Exposition. V06BT07A074.
- Kusiak, A., Song, Z., 2010. Design of wind farm layout for maximum wind energy capture. *Renew. Energy* 35, 685–694.
- Lackner, M.A., Elkinton, C.N., 2007. An analytical framework for offshore wind farm layout optimization. *Wind Eng.* 31, 17–31.
- Mosetti, G., Poloni, C., Diviacco, B., 1994. Optimization of wind turbine positioning in large wind farms by means of a genetic algorithm. *J. Wind Eng. Ind. Aerod.* 51, 105–116.
- Nazir, M.S., Mahdi, A.J., Bilal, M., Sohail, H.M., Ali, N., Iqbal, H.M., 2019. Environmental impact and pollution-related challenges of renewable wind energy paradigm—a review. *Sci. Total Environ.* 683, 436–444.
- Pérez-Arancí, J., Casillas-Pérez, D., Jiménez-Fernández, S., Prieto-Godino, L., Salcedo-Sanz, S., 2022. A versatile multi-method ensemble for wind farm layout optimization. *J. Wind Eng. Ind. Aerod.* 225, 104991.
- Pillai, A., Chick, J., Johanning, L., Khorasanchi, M., De Laleu, V., 2015. Offshore wind farm electrical cable layout optimization. *Eng. Optim.* 47, 1689–1708.
- Tao, S., Xu, Q., Feijóo, A., Zheng, G., Zhou, J., 2020a. Nonuniform wind farm layout optimization: a state-of-the-art review. *Energy* 209, 118339.
- Tao, S., Xu, Q., Feijóo, A., Zheng, G., Zhou, J., 2020b. Wind farm layout optimization with a three-dimensional Gaussian wake model. *Renew. Energy* 159, 553–569.
- The MathWorks Inc, 2022a. fmincon SQP Algorithm. <https://www.mathworks.com/help/optim/ug/constrained-nonlinear-optimization-algorithms.html#bsggpl4>.
- The MathWorks Inc, 2022b. How the Genetic Algorithm Works. <https://www.mathworks.com/help/gads/how-the-genetic-algorithm-works.html>.
- Ti, Z., Deng, X.W., Yang, H., 2020. Wake modeling of wind turbines using machine learning. *Appl. Energy* 257, 114025.
- Ti, Z., Deng, X.W., Zhang, M., 2021. Artificial Neural Networks based wake model for power prediction of wind farm. *Renew. Energy* 172, 618–631.
- van der Laan, M., Sørensen, N.N., Réthoré, P.-E., Mann, J., Kelly, M.C., Schepers, J., 2013. Nonlinear Eddy Viscosity Models Applied to Wind Turbine Wakes. Proceedings for the ICOWES2013, Copenhagen, Denmark, pp. 514–525.
- Van Der Laan, M.P., Sørensen, N.N., Réthoré, P.E., Mann, J., Kelly, M.C., Troldborg, N., Schepers, J.G., Machefaux, E., 2015. An improved k-e model applied to a wind turbine wake in atmospheric turbulence. *Wind Energy* 18, 889–907.
- Van Soest, H.L., den Elzen, M.G., van Vuuren, D.P., 2021. Net-zero emission targets for major emitting countries consistent with the Paris Agreement. *Nat. Commun.* 12, 1–9.
- Wan, C., Wang, J., Yang, G., Zhang, X., 2010. Optimal micro-siting of wind farms by particle swarm optimization. In: International Conference in Swarm Intelligence, pp. 198–205. Springer.
- Wang, L., Tan, A.C., Gu, Y., 2015. Comparative study on optimizing the wind farm layout using different design methods and cost models. *J. Wind Eng. Ind. Aerod.* 146, 1–10.
- Wang, L., Yuan, J., Cholette, M.E., Fu, Y., Zhou, Y., Tan, A.C., 2018. Comparative study of discretization method and Monte Carlo method for wind farm layout optimization under Weibull distribution. *J. Wind Eng. Ind. Aerod.* 180, 148–155.
- Wang, S., Wang, S., 2015. Impacts of wind energy on environment: a review. *Renew. Sustain. Energy Rev.* 49, 437–443.
- Wu, Y.-T., Porté-Agel, F., 2015. Modeling turbine wakes and power losses within a wind farm using LES: an application to the Horns Rev offshore wind farm. *Renew. Energy* 75, 945–955.
- Yang, Q., Hu, J., Law, S.-s., 2018. Optimization of wind farm layout with modified genetic algorithm based on boolean code. *J. Wind Eng. Ind. Aerod.* 181, 61–68.